Self-consistent theory of collective Brownian dynamics: Theory versus simulation

Laura Yeomans-Reyna,[1] Heriberto Acuña-Campa,[1] Felipe de Jesús Guevara-Rodríguez,[2] and Magdaleno Medina-Noyola[2,*]
[1]*Departamento de Física, Universidad de Sonora, Boulevard Luis Encinas y Rosales, 83000 Hermosillo, Sonora, Mexico*
[2]*Instituto Mexicano del Petróleo, Programa de Ingeniería Molecular, Eje Central Lázaro Cárdenas 152, 07730 México, Distrito Federal, Mexico*

(Received 3 June 2002; revised manuscript received 12 October 2002; published 26 February 2003)

A recently developed theory of collective diffusion in colloidal suspensions is tested regarding the quantitative accuracy of its description of the dynamics of monodisperse model colloidal systems without hydrodynamic interactions. The idea is to exhibit the isolated effects of the direct interactions, which constitute the main microscopic relaxation mechanism, in the absence of other effects, such as hydrodynamic interactions. Here we compare the numerical solution of the fully self-consistent theory with the results of Brownian dynamics simulation of the van Hove function $G(r,t)$ and/or the intermediate scattering function $F(k,t)$ of four simple model systems. Two of them are representative of short-ranged soft-core repulsive interactions [$(\sigma/r)^{\mu}$, with $\mu \gg 1$], in two and in three dimensions. The other two involve long-ranged repulsive forces in two (dipolar, r^{-3} potential) and in three (screened Coulomb, or repulsive Yukawa interactions) dimensions. We find that the theory, without any sort of adjustable parameters or rescaling prescriptions, provides an excellent approximate description of the collective dynamics of these model systems, particularly in the short- and intermediate-time regimes. We also compare our results with those of the single exponential approximation and with the competing mode-mode coupling theory.

DOI: 10.1103/PhysRevE.67.021108 PACS number(s): 05.40.−a, 83.80.Hj

I. INTRODUCTION

One of the most directly measurable dynamic phenomena of a colloidal dispersion is the relaxation of the fluctuations $\delta n(\mathbf{r},t)$ of the local concentration $n(\mathbf{r},t)$ of colloidal particles around its bulk equilibrium value n. The average decay of $\delta n(\mathbf{r},t)$ is described [1,2] by the time-dependent correlation function $\langle \delta n(\mathbf{r},t)\,\delta n(\mathbf{r}',0)\rangle$, referred to as the van Hove function $G(|\mathbf{r}-\mathbf{r}'|,t)$. This property can be determined directly by means of techniques such as digital video microscopy. Dynamic light scattering, on the other hand, measures directly the Fourier transform $F(k,t)$ of $G(r,t)$, referred to as the intermediate scattering function. This property contains, in principle, all the relevant dynamic information of the equilibrium suspension. Thus, the development of conceptually clear, and quantitatively accurate, statistical mechanical theories is required for the fundamental understanding of this important dynamic property.

With this aim, in recent work a self-consistent theory of colloid dynamics has been developed [3–5]. In the absence of hydrodynamic interactions, this scheme allows the calculation of $F(k,t)$ and its self-diffusion counterpart, $F_S(k,t)$, given the effective interaction pair potential $u(r)$ between colloidal particles, and the corresponding equilibrium static structure, represented by the radial distribution function $g(r)$ or the static structure factor $S(k)$ $[=F(k,t=0)]$. This theory, referred to as the self-consistent generalized Langevin equation (SCGLE) theory, is based on general and exact expressions for $F(k,t)$ and $F_S(k,z)$, in terms of a hierarchy of memory functions, derived within the generalized Langevin equation (GLE) approach and the process of contraction of the description, and complemented by a number of physically or intuitively motivated approximations. In its recent presentation in Ref. [3], this theory only referred to model monodisperse suspensions of spherical particles in the absence of hydrodynamic interactions, and its quantitative accuracy was tested through the comparison of its predictions for a specific idealized model system, with the corresponding Brownian dynamics computer simulation data. The same theoretical scheme is also being extended to describe colloidal mixtures, the effect of hydrodynamic interactions, and the ideal ergodic–nonergodic transition. A clear and simple discussion of these effects, however, will benefit from a systematic assessment of the intrinsic accuracy and limitations of the same theoretical scheme under the simplest possible conditions (model monodisperse suspensions of spherical particles with no hydrodynamic interactions).

For this reason, we have carried out a systematic comparison of the predictions of this theory and the corresponding computer simulation data for four idealized model systems. The first two are two-dimensional systems with power-law pair interaction, $\beta u(r)=A/r^n$, with $n=50$ (strongly repulsive, almost hard-disk-like) and with $n=3$ (long-range dipole-dipole interaction). The third one is the three-dimensional weakly screened repulsive Yukawa potential (whose two-dimensional version was studied in Ref. [3]). The last system considered involves short-ranged soft-core repulsive interactions. The dynamic equivalence between this and the strictly hard-sphere system allows us to discuss also the properties of the latter. For all these systems, we calculated $G(r,t)$ and/or $F(k,t)$ from the self-consistent theory, and performed Brownian dynamics simulations (without hydrodynamic interactions) to carry out extensive quantitative comparisons.

The aim of this exercise is to isolate the effects of the

*Permanent address: Instituto de Física Manuel Sandoval Vallarta, Universidad Autónoma de San Luis Potosí, Álvaro Obregón 64, 78000 San Luis Potosí, SLP, Mexico.

most important mechanism for the relaxation of the concentration fluctuations in colloidal liquids, namely, the nondissipative direct interaction forces between the colloidal particles. The quantitative theoretical description of these effects constitutes by itself a demanding and relevant challenge. We are interested, however, in a careful analysis of the predictions of this theoretical scheme under rather simple conditions, in order to have reliable information to be used as a reference in the development of this scheme into a more comprehensive theory that also includes the effects of hydrodynamic interactions, or the extension to colloidal mixtures.

Let us mention that the theory discussed here is certainly not the only proposal available of a fully self-consistent scheme for the collective and self-dynamics of colloidal suspensions. In fact, as early as in 1982, Hess and Klein [6] proposed the translation to colloids of the mode-coupling self-consistent theory of molecular liquids [7,8]. Although their proposal included an initial version of a fully self-consistent scheme for colloidal systems, only until recently extensive calculations based on such a theory were reported in the literature [9]. More recently, Nägele and collaborators have developed a more elaborate version of this mode-coupling theory specifically devised to deal with colloidal liquids [10]. The resulting self-consistent scheme has been extended and applied in several interesting directions [11], although only until recently the level of its quantitative accuracy at short and intermediate times has been documented [12,13]. The present theory shares with such proposal a number of important features, such as the prediction of the ideal glass transition [8] in a monodisperse system and the possibility of extension to more complex conditions. This is a consequence of the similarity in the mathematical structure of the resulting self-consistent schemes. As it was discussed in Ref. [3], however, the main difference of the proposal analyzed here, with respect to the various mode-coupling-based theories, lies in the conceptual framework upon which the former was built. Similarly, there is no direct relationship between the conceptual basis of the present theory and that of other theories of colloid dynamics partially or fully based on kinetic-theoretical concepts [14,15].

In what follows, we provide a brief summary of the SCGLE theory for colloid dynamics. In order for this paper to be reasonably self-contained, this will involve a certain degree of repetition with respect to Ref. [3]. For the reader interested in all the details and subtleties of the derivation of this theory, however, this summary is not a substitute of the direct consultation of Refs. [3–5], which describe the physical content and the rationale of each of the approximations involved in the present theory, and which explicitly monitor the quantitative accuracy of the most essential of them. The numerical solution of the resulting SCGLE scheme for four specific model systems, and their comparison with Brownian dynamics computer simulation data, constitute the main results of this work, and are reported in Secs. III through VI. In practice, the theory requires as an input the static structural properties [i.e., the radial distribution function $g(r)$ or the static structure factor $S(k)$] of the system. In order to avoid additional approximations, such as those involved in the use of approximate liquid-theory integral equations, these properties will also be provided by the computer simulations. All the simulation results reported in this paper correspond to Brownian dynamics simulation in the absence of hydrodynamic interactions, and at the beginning of Sec. III we summarize some relevant technical data of such simulations. Sections III and IV contain the comparison of theory and simulation for the two-dimensional systems with power-law pair interaction, $\beta u(r)=A/r^n$, with $n=50$ and with $n=3$, respectively. In Secs. V and VI we discuss, respectively, a similar comparison for the three-dimensional weakly screened repulsive Yukawa potential, and for a soft-core strongly repulsive potential at very high concentrations. The equivalence of the latter with the hard-sphere system is also discussed in Sec. VI. In Secs. V and VI, we also compare our results with those of other competing theories, particularly the mode-coupling scheme of Nägele and collaborators [12,13]. The main conclusions are summarized in Sec. VII.

II. SELF-CONSISTENT GLE THEORY

The self-consistent generalized Langevin equation theory discussed here, as originally presented in Ref. [3], is explicitly based on the formalization of two physically intuitive notions, namely, that collective diffusion should be related in a simple manner to self-diffusion, and that space-dependent self-diffusion, in its turn, should be related in a simple manner to the mean squared displacement (or some other k-independent self-diffusion property). The development of this theory involved four distinct fundamental elements. The first consists of the most general and exact expressions for $F(k,z)$ and $F_S(k,z)$ in terms of a hierarchy of memory functions. The general method (i.e., the generalized Langevin equation approach [16,17]) employed to derive such exact expressions has been explained and illustrated in Ref. [5].

The second element consists of the formalization of the notion that collective dynamics should somehow be simply related to self-dynamics. Vineyard's approximation [18] is a simple (although qualitatively and quantitatively rather primitive [19,20]) implementation of this idea. This aspect was also discussed in all detail separately; thus, in Ref. [4], the general expressions for $F(k,z)$ and $F_S(k,z)$ in terms of higher-order memory functions were employed to propose and test a hierarchy of Vineyard-like approximations. Adopting any of these approximations reduces the problem of colloid dynamics to the determination of $F_S(k,z)$ or any of its memory functions.

The third basic element of the present theory consists of the proposal for the approximate determination of $F_S(k,t)$. This step is also based on a physically intuitive expectation, namely, that space-dependent self-diffusion [represented by $F_S(k,t)$] should be simply related to the properties that characterize the Brownian motion of individual particles [1,6], just like in the Gaussian approximation, which expresses $F_S(k,t)$ in terms of the mean-squared displacement $W(t)$ as $F_S(k,t)=e^{-k^2W(t)}$. The present self-consistent theory introduces an analogous approximate connection between the functions $F_S(k,t)$ and $W(t)$, but at the level of their respective memory functions. The memory function of $W(t)$ is the so-called time-dependent friction function $\Delta\zeta(t)$. Thus, a fi-

nal ingredient in the development of the theory consists of an expression for $\Delta\zeta(t)$ in terms of $F(k,t)$ and $F_S(k,t)$ that results from the application of the generalized Langevin equation formalism to tracer-diffusion phenomena [16]. Such a closure relation finally determines our fully self-consistent theory of colloid dynamics. In what follows, we summarize the main results of Refs. [3–5], which contain, respectively, these four fundamental elements of the construction of the present theory.

In Ref. [5], the GLE approach, and the concept of the contraction of the description [16,17], was employed to derive the most general time-evolution equation for the fluctuations $\delta n(\mathbf{r},t)$ of a monodisperse colloidal suspension in the absence of hydrodynamic interactions. In such a derivation, the assumed underlying microscopic N-particle dynamics was provided by the many-particle Langevin equation [1]. As a result, expressions are derived for $F(k,t)$ and $F_S(k,t)$ [or their Laplace transforms $F(k,z)$ and $F_S(k,t)$] in terms of a hierarchy of memory functions, and of well-defined static structural properties of the Brownian fluid [5]. In these expressions, the Brownian relaxation time $\tau_B \equiv M/\zeta^0$ (or the corresponding frequency $z_B \equiv \tau_B^{-1}$) appears, where M and ζ^0 are, respectively, the mass and the solvent-friction coefficient of each particle in the suspension. In the absence of friction ($\zeta^0 \to 0$), these expressions correspond to those of a simple atomic liquid [20]. In the presence of friction, and in order to "tune" these expressions to the time regime normally probed by dynamic light scattering experiments, or by Brownian dynamics simulations, the limit $t \gg \tau_B$, or $z \ll z_B$, must be taken. Taking this so-called "overdamping" limit [6] requires a careful analysis, which was the main subject of Ref. [5]. As a result, one gets the most general expression for $F(k,t)$ and $F_S(k,t)$ that describes the dynamics of the suspension in the diffusive regime (i.e., for times $t \gg \tau_B$). The resulting "overdamped" expressions for $F(k,z)$ and $F_S(k,z)$ read, in Laplace space, as [5]

$$F(k,z) = \frac{S(k)}{z + \dfrac{k^2 D_0 S^{-1}(k)}{1 + C(k,z)}}, \tag{1}$$

$$F_S(k,z) = \frac{1}{z + \dfrac{k^2 D_0}{1 + C_S(k,z)}}, \tag{2}$$

where $C(k,z)$ and $C_S(k,z)$ are memory functions that, in turn, can be written in terms of the higher-order memory functions $\Delta L(k,z)$ and $\Delta L_S(k,z)$ as

$$C(k,z) = \frac{k^2 D_0 \chi(k)}{z + \chi^{-1}(k) L^0(k) + \chi^{-1}(k) \Delta L(k,z)} \tag{3}$$

and

$$C_S(k,z) = \frac{k^2 D_0 \chi_S(k)}{z + \chi_S^{-1}(k) L_S^0(k) + \chi_S^{-1}(k) \Delta L_S(k,z)}. \tag{4}$$

In these equations $D_0 = k_B T/\zeta^0$ is the free-diffusion coefficient of each particle ($k_B T$ being the thermal energy), $S(k)$ the static structure factor, and $\chi(k)$ the static correlation function of the fluctuations of the configurational component of the stress tensor of the Brownian fluid [notice that in Ref. [5] $\chi(k)$ and $\Delta L(k,z)$ carry a subindex "UU" that we shall drop systematically here]. $\chi(k)$ and $L^0(k)$, along with their self counterparts $\chi_S(k)$ and $L_S^0(k)$, are static properties, which can be written exactly [see Eqs. (A1) through (A4) of the Appendix] in terms of the two- and three-particle correlation functions, $g(r)$ and $g^{(3)}(\mathbf{r},\mathbf{r}')$, which are assumed to be known. In practice, the use of Kirkwood's superposition approximation allows us to write these properties in terms only of $g(r)$ [see Eq. (A6)]. Thus, the only unknowns in the expressions for $F(k,t)$ and $F_S(k,t)$ in Eqs. (1)–(4) are the memory functions $\Delta L(k,z)$ and $\Delta L_S(k,z)$.

We should mention that several authors, most recently Nägele and collaborators [10,11], have derived the results in Eqs. (1) and (2), using the projection operator formalism within the N-particle Smoluchowski dynamics. $C(k,z)$ and $C_S(k,z)$ are referred to as the normalized irreducible memory functions. The starting points of the approximate theory developed here are indeed these general results, but complemented with the additional information contained in Eqs. (3) and (4), which expresses the irreducible memory functions $C(k,z)$ and $C_S(k,z)$ in terms of the still higher-order memory functions $\Delta L(k,z)$ and $\Delta L_S(k,z)$.

Neglecting $\Delta L(k,z)$ and $\Delta L_S(k,z)$ in Eqs. (3) and (4) leads to the so-called single exponential (SEXP) approximation [21,22], that consists of Eqs. (1) and (2) with

$$C(k,z) \approx C^{\mathrm{SEXP}}(k,z) \equiv \frac{k^2 D_0 \chi(k)}{z + \chi^{-1}(k) L^0(k)} \tag{5}$$

and

$$C_S(k,z) \approx C_S^{\mathrm{SEXP}}(k,z) \equiv \frac{k^2 D_0 \chi_S(k)}{z + \chi_S^{-1}(k) L_S^0(k)}. \tag{6}$$

This approximation is exact at short times and/or large wave vectors, and constitutes a simple but nontrivial zeroth-order level of approximation of the self-consistent theory discussed here, which involves nonzero memory functions $\Delta L(k,z)$ and $\Delta L_S(k,z)$.

The second element in the construction of this theory is the proposal of an approximate relationship between $F(k,t)$ and $F_S(k,t)$. Vineyard's approximation consists of the simplest of such relations, in which $F(k,t)$ is approximated directly by $F_S(k,t)S(k)$. In Ref. [4], we performed a detailed numerical study of alternative, more sophisticated manners to refer collective dynamics to self-diffusion. Rather than relating $F(k,t)$ directly to $F_S(k,t)$, we proposed to approximate a given memory function of $F(k,t)$ by the corresponding memory function of $F_S(k,t)$. As an illustration, consider Eqs. (1)–(4). This suggests to relate $F(k,z)$ to $F_S(k,z)$ through their highest-order memory functions $\Delta L(k,z)$ and $\Delta L_S(k,z)$. The detailed manner in which this is done turns out to be important, as it was discussed in Ref. [4], where it

was shown that the most accurate and fundamental proposal for a Vineyard-like connection between $F(k,z)$ and $F_S(k,z)$, among the ones that can be suggested by the general results in Eqs. (1)–(4), is defined through the following approximation:

$$\frac{\Delta L(k,z)}{L^0(k)} = \frac{\Delta L_S(k,z)}{L_S^0(k)}. \tag{7}$$

Taken together with Eqs. (1)–(4), this equation defines an approximate scheme that allows us to express $F(k,z)$ and $F_S(k,z)$ in terms of a single normalized memory function, namely, $\Delta L_S(k,z)/L_S^0(k)$. One reason for the accuracy of this Vineyard-like approximation is the fact that the use of the exact results in Eqs. (1)–(4) guarantees that, independently of the value of $\Delta L(k,z)$ and $\Delta L_S(k,z)$, the resulting expressions for $F(k,t)$ and $F_S(k,t)$ will satisfy exactly the first three (short-time) moment conditions [23,24].

In practice, however, in Ref. [3] and in this work we employ a Vineyard-like relation between $F(k,z)$ and $F_S(k,z)$ which is defined in terms of a simple connection between the memory functions $C(k,z)$ and $C_S(k,z)$, but which happens to be just as accurate as the most sophisticated proposal in Eq. (7). This Vineyard-like approximation also preserves the exact short-time behavior up to order t^3 for $F(k,t)$ and $F_S(k,t)$, and is defined by the general results in Eqs. (1) and (2), along with the following approximate relation [4]:

$$\frac{C(k,z)}{C^{\mathrm{SEXP}}(k,z)} = \frac{C_S(k,z)}{C_S^{\mathrm{SEXP}}(k,z)}, \tag{8}$$

where $C^{\mathrm{SEXP}}(k,z)$ and $C_S^{\mathrm{SEXP}}(k,z)$ are given, respectively, by Eqs. (5) and (6). Just like the previous higher-order Vineyard-like approximation, this scheme refers both $F(k,z)$ and $F_S(k,z)$, through Eqs. (1), (2), and (8), to the knowledge of a single memory function, namely, $C_S(k,z)$. Thus, the remaining problem is to find some form of approximation for this memory function.

In contrast to the previous elements of the construction of the present theory, which are the straightforward formalization of two intuitive physical expectations, we do not have a similarly transparent physical notion to guide us in the construction of an approximate expression for this memory function. We know, however, two exact limits that $C_S(k,z)$ must satisfy. Thus, for large wave vectors, $C_s(k,z)$ is given exactly by $C_s^{\mathrm{SEXP}}(k,z)$, whereas for small wave vectors, $C_s(k,z)$ is given exactly by the Laplace transform, $\Delta\zeta(z)$, of a function $\Delta\zeta(t)$, referred to as the time-dependent friction function. For $\Delta\zeta(t)$, a general approximate expression has also been derived within the framework of the GLE approach [16]. This expression is

$$\Delta\zeta(t) = \frac{k_B T n}{(2\pi)^3 \zeta^0} \int d\mathbf{k} \frac{[k_z h(k)]^2}{1+nh(k)} F(k,t) F_S(k,t). \tag{9}$$

Thus, in Ref. [3] it was proposed to interpolate $C_S(k,z)$ between these two exact limits by means of the following expression:

$$C_S(k,z) = C_S^{\mathrm{SEXP}}(k,z) + [\Delta\zeta(k) - C_S^{\mathrm{SEXP}}(k,z)]\lambda(k), \tag{10}$$

where $\lambda(k)$ is a phenomenological interpolating function such that $\lambda(k)\to 1$ for $k\to 0$, and $\lambda(k)\to 0$ for $k\to\infty$. In Ref. [3], a functional form of the general type $\lambda(k) = [1 + (k/k_c)^{\nu}]^{-1}$ was proposed, and the choice of the parameters k_c and ν was made by comparing the theoretical predictions for various values of k_c and ν with exact (computer simulated) data for a particular model system, at a given state, and at a given time. This led to the following prescription for $\lambda(k)$:

$$\lambda(k) = \frac{1}{1+\left(\frac{k}{k_{\min}}\right)^2}, \tag{11}$$

where $k_{\min}$ is the position of the first minimum of the static structure factor $S(k)$ of the system.

The self-consistent scheme that results from all the arguments and approximations above can then be summarized by Eqs. (1), (2), (8)–(11). In Ref. [3], it was shown that the predictions of this scheme tuned out to be highly accurate for other times and other states of the same model system (two-dimensional repulsive Yukawa Brownian fluid) employed to calibrate the parameters k_c and ν of the interpolating function $\lambda(k)$. As we demonstrate now, the level of accuracy of the same theory, with $\lambda(k)$ now fixed by the same prescription in Eq. (11), continues to be equally accurate, at least when applied to other representative model systems, like the ones studied in the following sections.

In reference to the relatively arbitrary choice of a particular functional form for $\lambda(k)$, we may say that this corresponds, for example, to the choice of a particular vertex function in the self-consistent theories derived within the well-known mode-coupling approaches [6–13]. Also in that theory, a sensible guess of the right vertex function must compensate our otherwise fundamental ignorance of the detailed manner in which the many-body microscopic dynamics determines the macroscopic laws that describe the experimentally observed behavior of our system.

The self-consistent scheme consisting of Eqs. (1), (2), and (8)–(11) has to be solved numerically. As an input, we employ the computer-simulated radial distribution function $g(r)$ for the desired pair potential, and then calculate all the corresponding static properties $[S(k), \chi(k), L^0(k), \chi_S(k)$, and $L_S^0(k)]$, as described in the Appendix. Equations (1), (2), (8), and (10) are then written in t space as a set of coupled integro-differential equations involving the dimensionless wave vector variable $k\sigma$ and time variable t/t_0, with $t_0 \equiv \sigma^2/D_0$, σ being the particle diameter. The functions of k and t are then discretized in a mesh of points large enough to ensure independence of the solution with respect to the size of the mesh. The solution of the discretized system of equations is solved by a straightforward direct iteration method. The corresponding numerical solutions are presented in the following sections.

TABLE I. Simulation parameters. First column, soft disk system (SD) (studied in Sec. III), dipole-dipole system (DD), Yukawa potential with Gaylor *et al.* parameters (G), Yukawa potential with Härtl *et al.* parameters (H), Soft sphere system (SS), and hard sphere system (HS). In each case N is the number of particles, ϕ the volume fraction, Δt^* the dimensionless time step, NC the number of configurations for statistical properties, and TC is the total number of configurations.

System	N	ϕ	Δt^*	NC	TC
SD	500	0.3927	4.9×10^{-7}	8.0×10^{3}	1.615×10^{8}
DD	1000	0.0322	6.95×10^{-5}	8.0×10^{3}	8.3×10^{5}
G	800	0.00044	4.48×10^{-4}	4.0×10^{3}	4.15×10^{5}
H	800	0.000524	1.0×10^{-3}	4.0×10^{3}	4.15×10^{5}
SS	338	0.5146	1.6397×10^{-5}	5.5×10^{5}	5.5×10^{5}
HS	305	0.465		7.36×10^{7}	9.2×10^{7}

III. TWO-DIMENSIONAL SYSTEM WITH STRONGLY REPULSIVE FORCES

The first model system we consider is a two-dimensional Brownian fluid system with strongly repulsive interactions, determined by the pair potential

$$\beta u(r)=\frac{6}{(r/\sigma)^{50}}. \tag{12}$$

The reason we studied in detail this particular model system is that it constitutes a reasonable representation of a hard-core system by a steep, but continuous, pair potential. For the latter, we can calculate some properties [the short-time moment conditions of $F(k,t)$, for example], that do not exist for a discontinuous potential. In addition, exactly this model system was found to fit the experimentally determined structure of a real quasi-two-dimensional suspension studied by Santana-Solano and Arauz-Lara [25]. Here, however, we only wish to compare the time evolution of $G(r,t)$, as predicted by the SCGLE theory, with that determined by Brownian dynamics computer simulations.

Our Brownian dynamics simulations follow the rather conventional approach based on the Ermak-McCammon algorithm with periodic boundary conditions [26–28]. The simulation results presented in this paper were produced after we made a careful choice of the size of the cubic simulation cell, the number of particles, the time step, the length of the run, etc., so as to eliminate any artificial dependence on these parameters. In Table I we summarize the values of these parameters, corresponding to the simulation of the four systems considered in this paper.

Figure 1 exhibits $G(r,t)$ for the model system in Eq. (12) at a reduced concentration $n^*=n\sigma^2=0.50$ ($\phi=\pi n^*/4=0.3927$) and for two times representative of the short- and intermediate-time regimes. For the system in Fig. 1, the only relevant length scales are the diameter σ and the mean interparticle distance $l=n^{-1/2}$, whose ratio $l^*\equiv l/\sigma=(n^*)^{-1/2}\approx1.4$. Thus, the mean collision time t_c can be estimated through the relation $(l-\sigma)^2\approx4D_0t_c$ (where D_0 is the free diffusion coefficient), and is given by $t_c\approx[(n^*)^{-1/2}-1]^2t_0/4$, with $t_0\equiv\sigma^2/D_0$. Thus, for the system we are discussing, $t_c/t_0\approx0.04$. This is the time scale that defines the intermediate-time regime illustrated in Figs. 1(a) and 1(b), which presents $G(r,t)$ for two times, $t/t_0=0.01$ and $t/t_0=0.06$. Figure 1(a) illustrates the high degree of accuracy on the SCGLE theory, which overlaps completely with the simulation data. This is indeed expected, since the SCGLE theory has built-in exact short-time behavior [3]. In fact, for these early times, the SEXP, which is a much simpler theory [21,22], is almost equally accurate [dashed line in Fig. 1(a)]. For the longer time in Fig. 1(b), however, the differences between the SCGLE theory and the SEXP approximation are now much more appreciable, mostly at small distances, and becomes negligible at longer distances. For all distances, however, the SCGLE theory virtually overlaps with the simulation data (at small values of r, the accuracy of the simulation results becomes increasingly poorer, due to poor statistics, and this is the source of the deviations between the SCGLE theory and the simulation data near $r=0$).

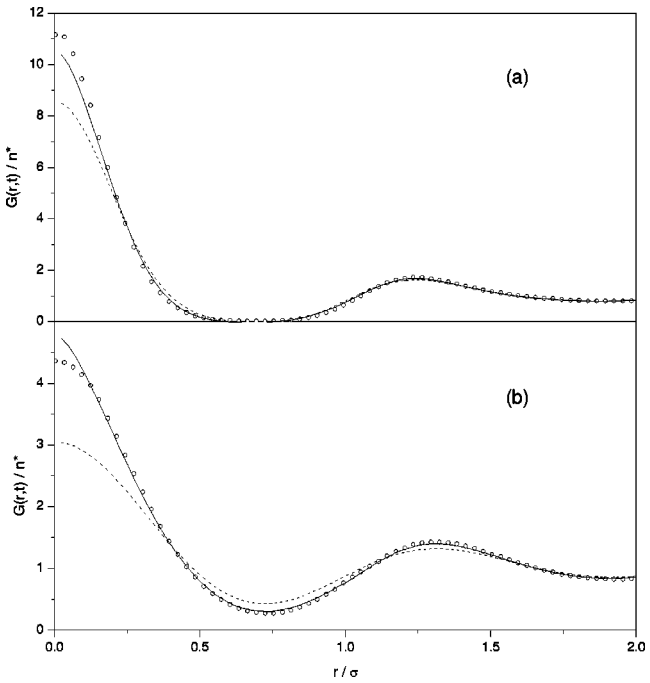

FIG. 1. van Hove function $G(r,t)$ of the Brownian fluid with pairwise interactions given by Eq. (12) at $n^*=0.5$ at (a) $t/t_0=0.01$ and (b) $t/t_0=0.06$. SCGLE theory (solid line), SEXP theory (dashed line), and Brownian dynamics (BD) simulation results (symbols).

In order to illustrate the relaxation of concentration fluctuations for the same system, but now in Fourier space, in Fig. 2 we compare the static structure $S(k)$, which is the initial value $F(k,t=0)$ of the intermediate scattering function, with what remains after a time $t/t_0=0.06$ [the time corresponding to Fig. 1(b)]. In general, we found for other times, and also for other concentrations studied, what is illustrated in this figure, namely, that the predicted $F(k,t)$ matches the computer simulated $F(k,t)$ for all wave vectors, and that the largest disagreements occurs at the position $k_{\max}$ of the first peak of the static structure factor. Thus, a sum-

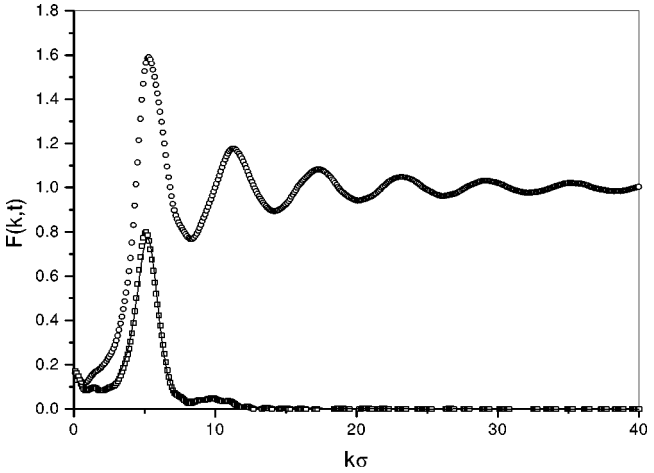

FIG. 2. Intermediate scattering function $F(k,t)$ for the system as in Fig. 1 at $t=0$ [i.e., the static structure factor $S(k)$] and $t/t_0=0.06$. SCGLE theory (solid line) and BD results (symbols).

mary of the comparisons discussed so far can be presented in terms of a comparison of the time evolution of the maximum $F(k_{\max},t)$ scaled with $S(k_{\max})$, as predicted by the SCGLE theory, with the computer simulation data. This summary is presented in Fig. 3. Notice that the predictions of the SCGLE continue to agree quite well with the simulation data for all times [Fig. 3 now includes times of the order of 2.5 times the mean collision time, at which there is almost no remnant of the initial structure $S(k)$].

The results presented in Figs. 1–3 allow us to conclude that the accuracy of the SCGLE theory is indeed quite good for this model system involving a hard-disk-like, but continuous, potential. In the following section we perform a similar analysis for a longer-ranged power-law potential.

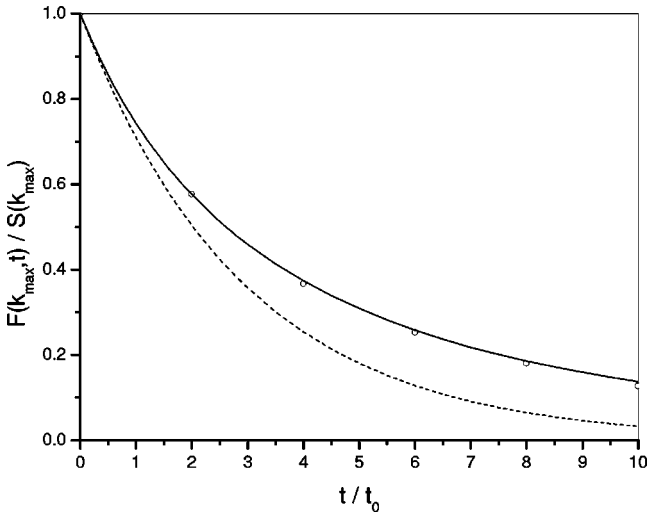

FIG. 3. Intermediate scattering function $F(k,t)$ normalized with $S(k)$ at the position $k_{\max}$ of the main peak of $S(k)$, as a function of dimensionless time t/t_0, for the same system as in Fig. 1. SCGLE theory (solid line), SEXP theory (dashed line), and BD simulation results (symbols).

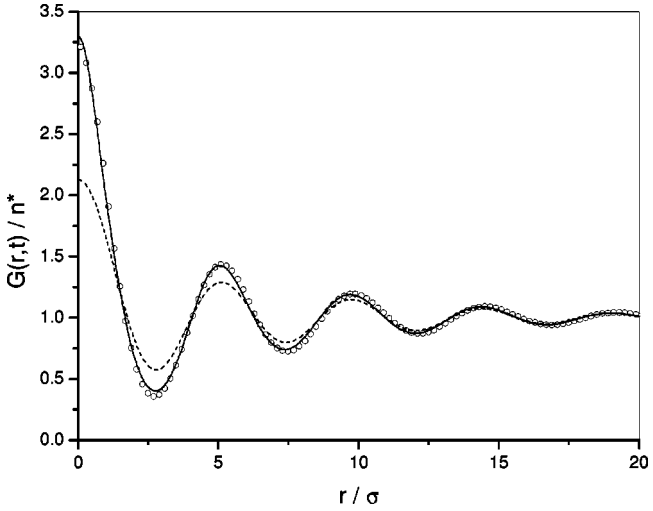

FIG. 4. van Hove function $G(r,t)$ for the Brownian fluid with pairwise interactions given by Eq. (14) with $\Gamma=4.4$ and $n^*=0.041$ at $t/t_0=1.666$. SCGLE theory (solid line), SEXP theory (dashed line), and BD results (symbols).

IV. TWO-DIMENSIONAL SYSTEM WITH DIPOLE-DIPOLE (R^{-3}) INTERACTIONS

In this section we discuss the results of the SCGLE theory for the dynamics of another two-dimensional system, this time with long-ranged repulsive interactions. This model system corresponds, as far as the interaction forces is concerned, to the quasi-two-dimensional system of paramagnetic colloidal particles studied by Zahn *et al.* [29]. We define this system by the pair potential

$$\beta u(r)=\begin{cases} A/r^3, & r>\sigma \\ \infty, & r<\sigma \end{cases} \tag{13}$$

and by its number concentration (per unit area) n. The specific conditions that we shall consider correspond to a very dilute suspension according to the reduced number concentration $n^*=n\sigma^2$, which will be $n^*=0.041$ ($\phi=\pi n^*/4=0.0322$). In contrast, the amplitude A/σ^3 of the dipolar interaction at hard-core contact will be large enough [$\beta u(r=\sigma)\approx 530$], so that, in reality, hard-disk contact is prevented by the strong dipole-dipole repulsion. Thus, the only meaningful term in the interaction potential is the dipole-dipole term, which can also be written as

$$\beta u(r)=\frac{\Gamma}{(r/l)^3}, \tag{14}$$

where $\Gamma=A/l^3$, with $l=n^{-1/2}$. For the conditions considered here, $\Gamma=4.4$.

For this system we also calculated theoretically $G(r,t)$ and $F(k,t)$ for short and intermediate times, and compared them with the corresponding simulation data. The scenario turns out to be quite similar to that described for the system of the preceding section, concerning the general accuracy of the SCGLE theory. Thus, Fig. 4 illustrates a comparison typical of the intermediate-time regime ($t/t_0=1.666$, with t_0

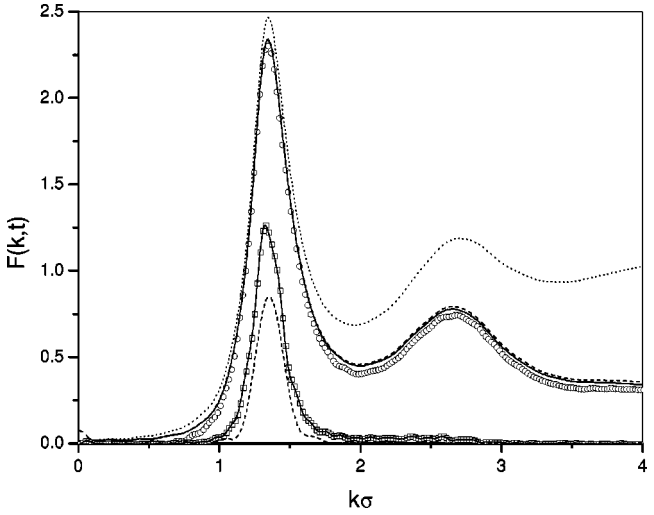

FIG. 5. Intermediate scattering function $F(k,t)$ for the same system as in Fig. 4 at $t=0$ [static structure factor $S(k)$, dotted line], $t/t_0=0.0833$, and $t/t_0=1.666$. SCGLE theory (solid line), SEXP theory (dashed line), and BD simulation results (symbols).

$=\sigma^2/D_0$). This figure, as well as Fig. 5, also includes the results of the SEXP approximation. For the conditions of Fig. 4, the limitations of this simpler theory are already quite evident. Figure 5 includes the information of Fig. 4, but in Fourier space, as well as $F(k,t)$ for another, shorter, time $(t/t_0=0.0833t_0)$. For reference, the static structure factor $S(k)=F(k,t=0)$ is also included in this figure. Figures 4 and 5 illustrate the high accuracy of the SEXP theory at short times, and the excellent level of accuracy of the SCGLE results for $F(k,t)$ in the intermediate-times regime for all wave vectors. In Fig. 6, we compare the theoretical predictions for the decay of the main peak of $F(k,t)$ with the simulation data for a longer time span.

This comparison indicates that although there are small systematic differences with respect to the exact (simulation) data, these are not appreciable within the resolution of Figs. 4–6. Thus, the SCGLE theory continues to provide an excellent quantitative description of the relaxation of the concentration fluctuations for times well beyond the intermediate-time regime. We may recall that the corresponding differences were also virtually negligible in the case of the two-dimensional repulsive Yukawa system that was employed in Ref. [3] to illustrate the quantitative application of the SCGLE theory. That system, however, was precisely the system employed to calibrate the only element of the theory that could not be determined from more basic principles, namely, the interpolating function $\lambda(k)$ of Eq. (11). The SCGLE results for both two-dimensional model systems studied in this and in the preceding section involve neither a different interpolating function nor additional or specific calibration procedures: here we employed the same interpolating function determined in Ref. [3], namely, Eq. (11). Our present comparisons simply show that this continues to be an excellent choice of $\lambda(k)$ also for both of these additional two-dimensional model systems.

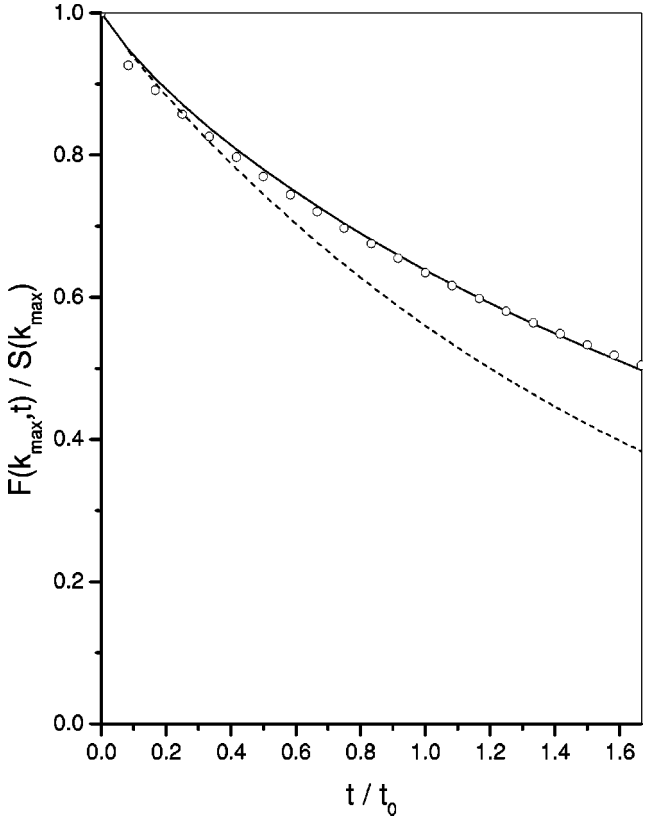

FIG. 6. Intermediate scattering function $F(k,t)$ normalized with $S(k)$ at the position $k_{\max}$ of the main peak of $S(k)$ as a function of t/t_0 for the same system as in Fig. 4. SCGLE theory (solid line), SEXP theory (dashed line), and BD results (symbols).

V. THREE-DIMENSIONAL REPULSIVE YUKAWA POTENTIAL

In this section we present a similar comparison, but this time involving a relevant three-dimensional system, namely, the repulsive Yukawa potential,

$$\beta u(r)=\begin{cases} K\dfrac{e^{-z(r/\sigma-1)}}{(r/\sigma)}, & r>\sigma \\ \infty, & r<\sigma. \end{cases} \tag{15}$$

This corresponds to the electrostatic contribution of the well-known Derjaguin-Landau-Verwey-Overbeek potential [30,31]. Here we consider the regime of strong electrostatic repulsion $(K\gg 1)$ and weak screening $(z=\varkappa\sigma<1)$, so that the hard-sphere diameter, as in the previous example, is only an arbitrary unit length of no physical significance.

We have compared the theoretical predictions of our theory with the corresponding Brownian dynamics (BD) computer simulations for several values of the parameters K and z of this system, and for various concentrations that we express in terms of the volume fraction $\varphi\equiv\pi n\sigma^3/6$. In all these comparisons, which we do not report in detail, we observe the same scenario, which we illustrate here for two particular sets of parameters, for which Brownian dynamics simulations have been reported in the literature. The first corresponds to the parameters $K=556$, $z=0.149$, and φ

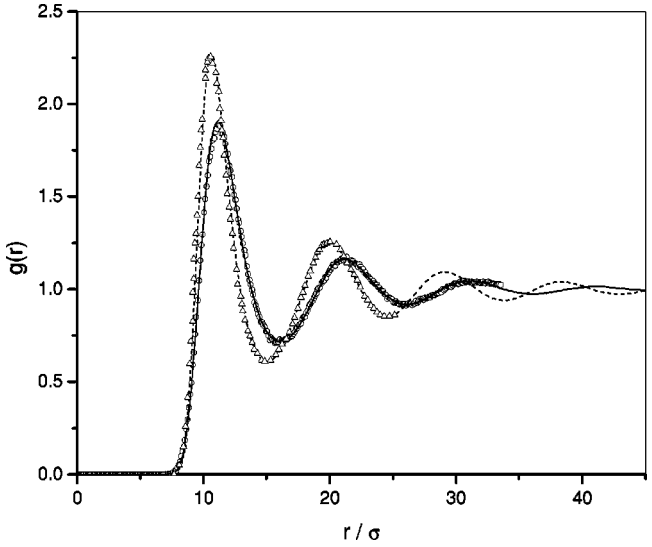

FIG. 7. Simulated radial distribution function $g(r)$ for the repulsive Yukawa potential. Open circle and solid line: $K=556$, $z=0.149$, and $\phi=4.4\times10^{-4}$ studied by Gaylor *et al.* (Ref. [28]); open triangle and dashed line: $K=1002.74$, $z=0.222$, and $\phi=5.24\times10^{-4}$ studied by Härtl *et al.* (Ref. [32]).

$=4.4\times10^{-4}$, employed by Gaylor *et al.* [28], and the second to the parameters of the system studied by Härtl *et al.* [32], namely, $K=1002.74$, $z=0.222$, and $\varphi=5.24\times10^{-4}$.

As a matter of elementary routine checking of our own BD simulations, in both cases we first reproduced the reported simulation runs, and verified the full agreement between the reported results for $G(r,t)$ and our reproduction run. We then performed a second run with a much larger number of particles (but otherwise with the same parameters as the original runs). The new results for $G(r,t)$, $G_s(r,t)$, and $G_d(r,t)$ did not differ from those of the previous runs. However, they extended the range in r to improve the fit of the asymptotic tails, and hence, the accuracy of the Fourier transforms to get the intermediate scattering functions. Figure 7 compares the results of both runs for the radial distribution functions of the two systems. This structural information was also the static input in the calculation of the results of the SCGLE theory. Similar agreement as in Fig. 8 was observed between the results for $G(r,t)$ of the two runs for all the nonzero times reported below.

In Fig. 8 we compare the theoretical and the simulation results for the intermediate scattering function for the system of Gaylor *et al.* Let us first say that we found a slight difference between our simulation data for $F(k,t)$ and the reported results of Gaylor *et al.*, particularly near the main peak. These differences are illustrated in Fig. 8, where we also include the data of Gaylor *et al.* (as digitized from Fig. 1 of Ref. [12]), for the shortest and the longest nonzero times considered in the figure. These differences are due to the different accuracy of the processing of the data for $G(r,t)$ to get $F(k,t)$. This must be considered in drawing conclusions from a comparison of theoretical results with computer simulation data for $F(k,t)$. The conclusions that concern us here refer to the comparison of our theoretical results with our own, more precise, BD data for $F(k,t)$. From Fig. 8, we

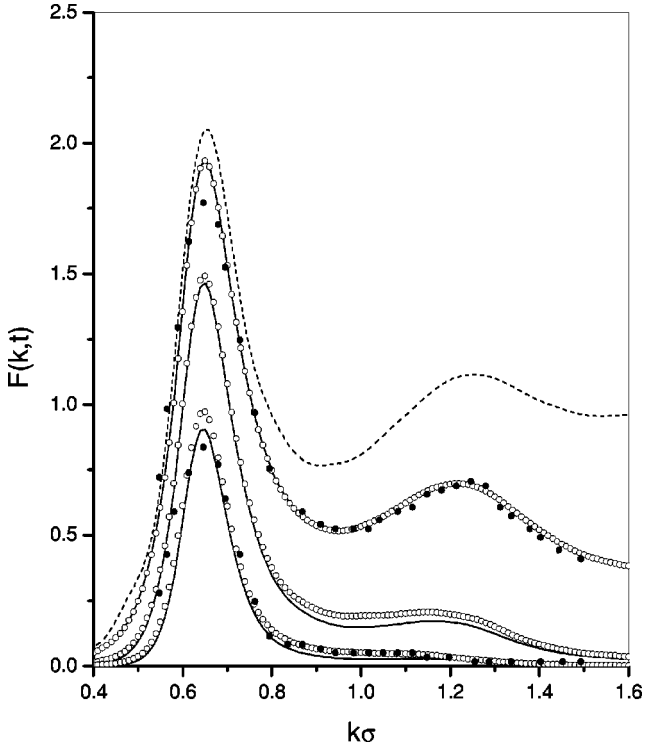

FIG. 8. Intermediate scattering function $F(k,t)$ for the repulsive Yukawa potential with $K=556$, $z=0.149$, and $\phi=4.4\times10^{-4}$ at $t=0$, 0.1, 0.6, and 1.6 ms. SCGLE theory (solid line), our BD simulation results (open circles), and $F(k,t)$ data taken from Gaylor *et al.* (filled circles).

conclude that our theory tends to relax somewhat faster than our BD simulation data at the main peak and at larger wave vectors. If we were to compare with the digitized data of Gaylor *et al.*, we would conclude the opposite, i.e., that our theoretical results at the main peak relax more slowly than the simulations. We should mention that Banchio *et al.* [12] compared their mode-coupling theory (MCT) results with the data of Gaylor *et al.*, with which they found complete agreement. Hence, according to the comparison in Fig. 8, their MCT results relax faster than our SCGLE predictions, and even faster than our more precise BD data. These conclusions, however, should not be taken as a definitive assessment of the relative accuracy of the MCT and the SCGLE theories, since the comparison is probably not fair for the MCT. This is because our SCGLE results involved the use of the exact static input in Fig. 7, whereas Banchio *et al.* employed the rescaled mean spherical approximation fit of the reported static structure factor of the data of Gaylor *et al.* for $S(k)$ as the static input of their MCT results.

Our current concern, however, is to learn and document the virtues and limitations of our SCGLE theory. For example, we can compare separately $F_s(k,t)$ and $F_d(k,t)$ with the corresponding BD data. This is done in Fig. 9. There we find that the theoretical predictions for $F_d(k,t)$ match the simulation results with a high degree of quantitative accuracy, whereas the results for $F_s(k,t)$ clearly exhibit a faster relaxation with respect to the BD data. Unfortunately, we cannot know if other theories will also exhibit similar quali-

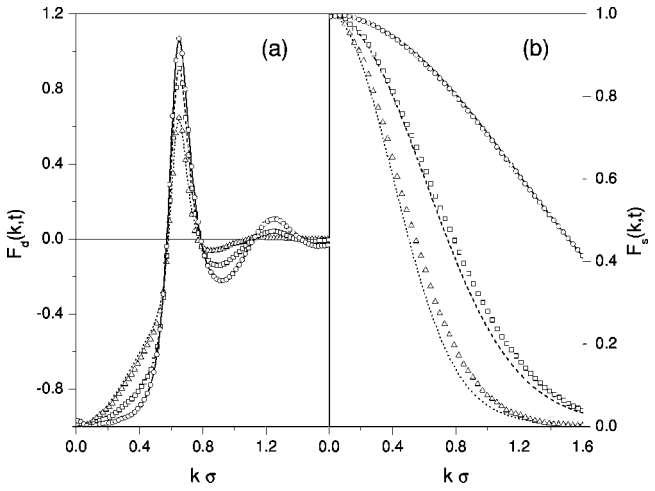

FIG. 9. Distinct and self parts of $F(k,t)$ for the system as in Fig. 8 at $t=0.1$, 0.6, and 1.6 ms. SCGLE theory (solid, dashed, and dotted lines) and BD simulation results (open circles, squares, and triangles).

tative features. In our case, however, this information could be used if attempts were made to quantitatively finetune the theory by means, for example, of a different prescription of the interpolating function $\lambda(k)$.

The system studied by Härtl *et al.* is clearly more structured than the one in the previous example, as can be appreciated from the comparison of the radial distribution functions in Fig. 7. However, we observed essentially the same scenario found for the system of Gaylor *et al.* for the intermediate scattering functions. What we report here is only the relaxation of $F(k,t)$ as a function of time at two fixed wave vectors ($k\sigma=0.60$ and 0.69, the latter corresponding to the position of the main peak of the static structure factor), for which Härtl *et al.* report BD data, and Banchio *et al.* report MCT results. This is done in Fig. 10. Our BD data in this figure derive from the second, more accurate run. Comparing the SCGLE results with our data, we see that there is quite an acceptable quantitative agreement. In Fig. 10 we also include the MCT results and the BD data of Härtl *et al.*, read from Fig. 2(b) of Ref. [12]. Again, there are some discrepancies in both sets of simulation data, particularly for the smaller wave vector, and the MCT results are favored by our new, more precise BD data at the main peak, but not at the other wave vector.

In summary, the comparisons in this section indicate that our self-consistent theory provides a reliable description of the dynamics of the three-dimensional Yukawa Brownian fluid. The actual quantitative accuracy is not as perfect as in the case of the two-dimensional Yukawa system, or of the other two-dimensional systems studied in this work. However, the idea here was to apply the same version of the SCGLE to systems other than the specific two-dimensional system for which the theory was initially calibrated.

VI. THREE-DIMENSIONAL SYSTEM WITH STRONGLY REPULSIVE FORCES

In this section we consider a three-dimensional system of Brownian particles interacting through some form of soft,

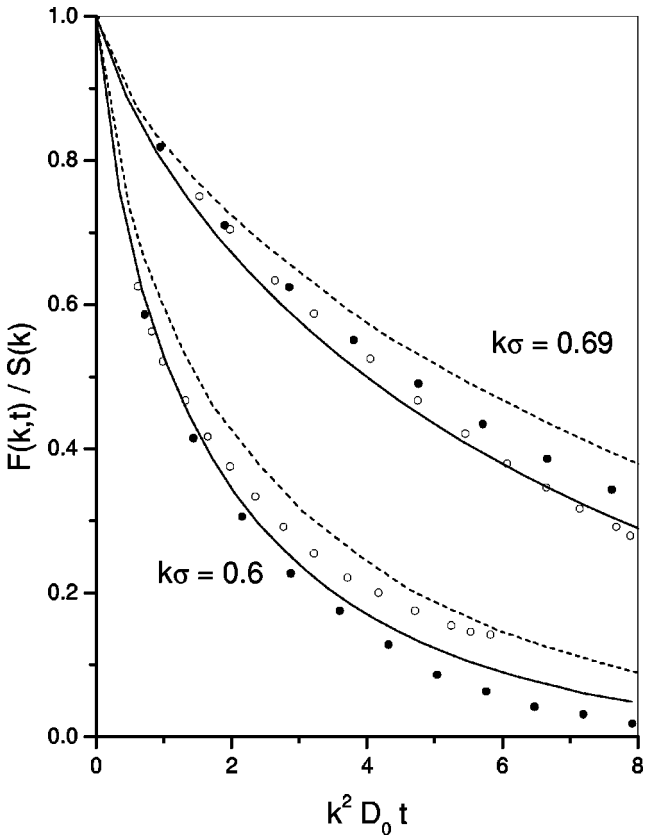

FIG. 10. Intermediate scattering function $F(k,t)$ normalized with $S(k)$ for $k\sigma=0.60$ and $k\sigma=0.69$ as a function of k^2D_0t, for the repulsive Yukawa potential studied by Härtl. SCGLE theory (solid lines), MCT theory (dashed lines), BD simulations taken from Härtl *et al.* (Ref. [32]) (open circles), and our BD results (filled circles).

but strongly repulsive and short-ranged, pair potential $u(r)$. For our present purpose, the particular form of this potential is irrelevant. For concreteness, however, we choose to write it as

$$\beta u(r)=\frac{1}{(r/\sigma_s)^{2\nu}}-\frac{2}{(r/\sigma_s)^{\nu}}+1 \qquad (16)$$

for $0<r<\sigma_s$, and assume that it vanishes for $r>\sigma_s$. In this equation, ν is a positive integer. The only convenience of this particular functional form is that this potential and its derivative strictly vanish at, and beyond, σ_s, and that this family of soft-core potentials is being investigated in the context of a dynamic correspondence principle that allows one to simulate the properties of the hard-sphere (HS) system in the absence of hydrodynamic interactions. In this section we only consider the specific case $\nu=18$, at a soft-sphere volume fraction $\phi_s\equiv\pi n\sigma_s^3/6=0.5146$.

In Fig. 11 we present the static input employed in the theoretical calculations of the dynamics of this system. The radial distribution function in Fig. 11(a) is the result of the Brownian dynamics simulation for the soft-sphere potential above. In Table I we provide the technical parameters of the simulation procedure. This is also based on the conventional

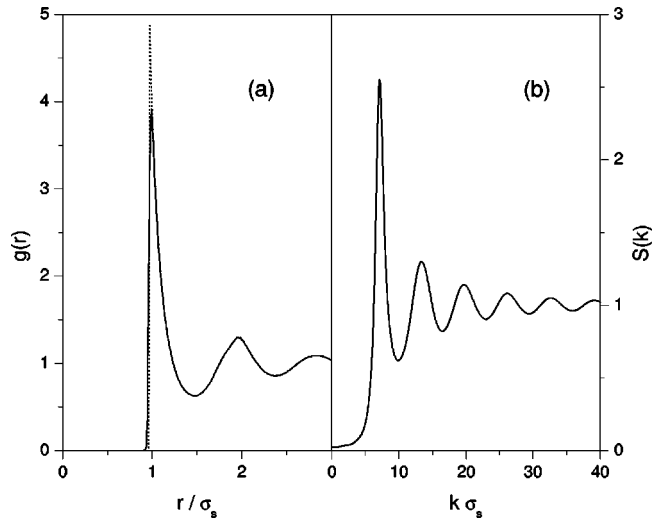

FIG. 11. (a) Simulated radial distribution function $g(r)$ for the soft sphere potential in Eq. (16) with $\nu=18$ and $\phi=0.5146$ (solid line), and for a hard sphere system with $\phi=0.465$ (dashed line); (b) static structure factor for the soft sphere system.

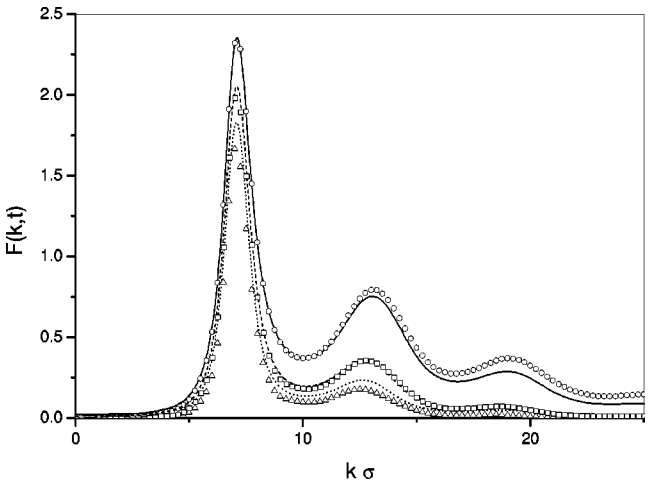

FIG. 12. Intermediate scattering function $F(k,t)$ for the soft sphere system as in Fig. 11 at $t/t_0=0.006\,559,\ 0.026\,23,\ 0.052\,47$. SCGLE theory (solid, dashed, and dotted lines) and BD results (open circles, squares, and triangles).

Ermak-McCammon algorithm, which applies without special difficulties for the system under consideration. Figure 11(a) also includes the radial distribution function of the hard-sphere system at the same number concentration *n*, but with an effective diameter $\sigma_h=0.9667$, corresponding to a HS volume fraction of 0.465. This was obtained by means of an accurate Monte Carlo simulation, also described, in its technical details, in Table I. As we can see from Fig. 11(a), the static structure of these two systems is identical, except for a small region near the first maximum of $g(r)$. These differences, however, are virtually indistinguishable in the static structure factor, in the scale of Fig. 11(b). The static structure factor was calculated from the Fourier transform of the solid curve in Fig. 11(a), which is the fit of the actual simulation data for $g(r)$, extended to longer distances by the analytic tail suggested by Härtl *et al.*

With the static inputs in Fig. 11, we now solve our self-consistent scheme to calculate the van Hove function and its self and distinct parts for our soft-sphere system, as well as the (full, self, and distinct) intermediate scattering function. In Fig. 12 we illustrate the comparison between our theoretical results and the Brownian dynamics simulations for $F(k,t)$ at three different values of the correlation time (in units of $\tau_s\equiv\sigma_s^2/D^0$). We observe that our theory gives an initially excellent description of the decay of the main peak of $F(k,t)$, although at longer times this peak relaxes more slowly according to our theory, in comparison with the simulation data. For wave vectors beyond the first peak, on the other hand, the theoretical predictions are more inaccurate at all times; they first relax faster than the simulation data, and later they relax more slowly. Just for coincidence, at some intermediate time the agreement actually looks impressive. The sequence illustrated in the figure provides a precise assessment of the overall accuracy of our theory. A fair judgment of these comparisons, however, must take into account the fact that the conditions illustrated in this figure correspond to about 90% of the freezing volume fraction of our system, which is rather demanding for a theory that does not include any adjustable parameter or rescaling prescriptions of any sort.

Our theoretical scheme is, of course, open for improvement concerning its detailed quantitative accuracy, if such an aspect happens to be crucial. After all, there is nothing fundamental in the specific interpolating function $\lambda(k)$, which we chose not to touch in the calculation of all the results reported in this paper. If the situation would justify it, however, we can finetune this function through its specific calibration for the system of interest. Nevertheless, at this point the idea is to establish the virtues and limitations of our self-consistent scheme in its most rudimentary version. The device of any improved version, however, will benefit from the comparisons that our present Brownian dynamic results allow us to make.

For example, we can compare separately the self and the distinct parts of the intermediate scattering function. From such a comparison, we again discover that the theoretical predictions for the distinct part are far more accurate than the self and the full intermediate scattering functions, and they virtually superimpose on the corresponding BD data. The main source of the discrepancies seen in Fig. 12 for the full $F(k,t)$ then derives essentially from inaccuracies of its self part, which is illustrated in Fig. 13. This figure exhibits the same trend in $F_s(k,t)$ as observed in Fig. 12 in $F(k,t)$, namely, a faster decay at short times and large wave vectors, and a slower decay at long times, for all wave vectors. Although the inaccuracies of the theoretical results for the $F_s(k,t)$ could be removed to a large extent by an *ad hoc* calibration of the interpolating function, this is not the purpose of the work reported here.

More interesting is the fact that, upon a simple rescaling of the data, all that we have said so far in this section also refers to a hard-sphere system at a volume fraction of 0.465. In a separate communication, this dynamic equivalence be-

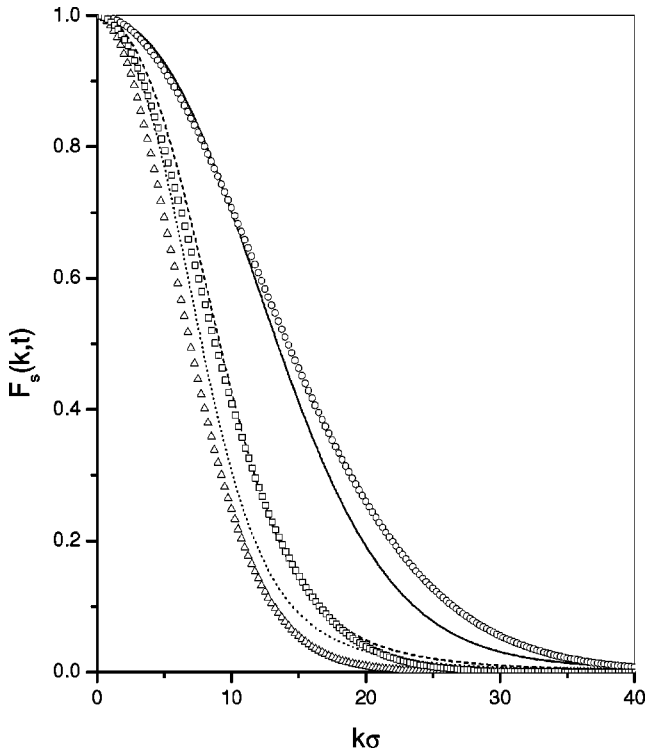

FIG. 13. Same as in Fig. 12, but for the self part of $F(k,t)$.

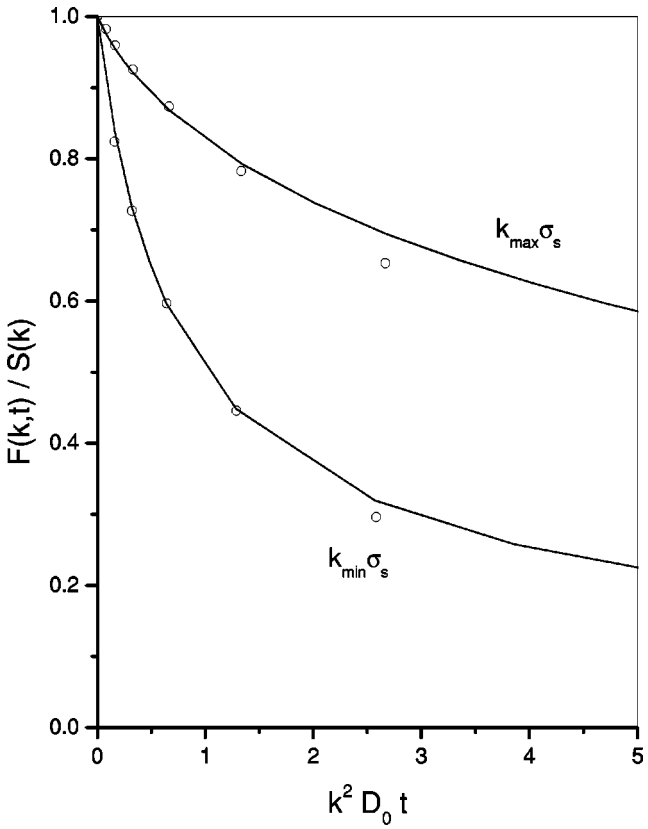

FIG. 14. Intermediate scattering function $F(k,t)$ normalized with $S(k)$ for $k_{\max}\sigma_s=7.13$ and $k_{\min}\sigma_s=9.92$ as a function of k^2D_0t for the soft sphere system as in Fig. 11. SCGLE theory (solid lines), and BD simulations results (open circles).

tween soft- and hard-sphere systems is demonstrated and proposed as an alternative algorithm to simulate the dynamics of a hard-sphere dispersion in the absence of hydrodynamic interactions [33]. Thus, in Fig. 14 we compare the decay of $F(k,t)$ for the same system at two fixed wave vectors corresponding to the position of the first maximum and the first minimum of the static structure factor. In terms of the dimensionless variables employed in Fig. 14, there is no need for any rescaling of the data in order for the same figure, which corresponds to a soft-sphere system at $\phi_s=0.5146$, to represent also the properties of a HS system at $\phi_h=0.465$. As we can see from this comparison, our theory provides quite a good description of the overall decay of the intermediate structure factor in the short- and intermediate-time regimes. We must say, however, that at much longer times, the slow relaxation of the self component leads to a poorer comparison, particularly at the main peak. This becomes more severe as the volume fraction is increased further. In fact, we also performed the same comparison as explained in this section for the soft-sphere volume fraction of $\phi_s=0.5534$, which corresponds to a HS system at $\phi_h=0.5$ (slightly above freezing). We find that our results for the decay of $F(k,t)$ at the minimum of the structure factor are in reasonable agreement with our own simulation data. We also checked that our BD data are also in agreement with those reported by Cichocki and Felderhof. Banchio *et al.* compared their rescaled MCT with such data and found very good agreement. Unfortunately, in neither of these works information is given for the decay at the position of the main peak of $S(k)$. In our case, we find that for such a case our theoretical results depart considerably from our BD data. A more detailed report of these comparisons, together with a discussion of their experimental relevance, will be given, however, in a separate communication [34].

VII. SUMMARY AND DISCUSSION

In this paper we have presented an extensive application of the SCGLE theory of colloid dynamics to a set of model suspensions without hydrodynamic interactions. In its original presentation, this theory was applied to a particular model system, namely, the two-dimensional repulsive Yukawa Brownian fluid. That application, however, also served to determine one element of the theory that could not be determined from more fundamental principles, namely, the interpolating function $\lambda(k)$ of Eq. (10). Thus, the doubt was left concerning the usefulness of that specific prescription for other systems, with the same or different dimensionality. The results presented in this paper illustrate the fact that this aspect of the theory should be of little concern. There are, indeed, small systematic deviations, particularly in the relaxation of $F(k,t)$ near its main peak, and these were illustrated in Figs. 3, 6, and 8. These deviations, however, only reflect the approximate nature of the theory, and exhibit the magnitude of the intrinsic accuracy of the approximations involved. One of them is precisely the particular functional form of the interpolation function $\lambda(k)$.

There is certainly no *a priori* reason to expect that the simple expression in Eq. (10) should have any form of universal character. However, the expectation that a given proposal for $\lambda(k)$, calibrated with a given model system, will work well for other systems turns out to be fulfilled to a satisfactory degree, according to the results reported in this paper. Let us mention that, besides the model systems reported here, we also performed similar exercises with additional pair potentials, including systems with an attractive potential well, with similar conclusions as those reported here.

We may say, in summary, that the SCGLE theory of colloid dynamics seems to be one of the most accurate quantitative theories for which extensive calculations have been performed for the collective diffusion properties of monodisperse suspensions in the absence of hydrodynamic interactions. Real suspensions exist for which hydrodynamic interactions may indeed be neglected, and for which the SCGLE theory should be directly applicable. The idea is, however, to employ what we have learned from the present exercise in the attempts to extend this theory to include the effects of hydrodynamic interactions. The results of such attempts will be reported separately [34].

ACKNOWLEDGMENTS

This work was supported by the Instituto Mexicano del Petróleo, through Grant No. FIES-98-101-1, and by the Consejo Nacional de Ciencia y Tecnología (CONACYT, México), through Grants Nos. G295589-E and NC0072: Materiales Biomoleculares. L.Y.R. and H.A.C. acknowledge the support of the Proyecto FOMES P/PIFI2001-26-FO-07 and from the Área de Cómputo de Alto Rendimiento (ACAR) of the Universidad de Sonora (UNISON, México). M. Medina-Noyola acknowledges the kind hospitality of the Departamento de Física del Centro de Investigación y de Estudios Avanzados del Instituto Politécnico Nacional (CINVESTAV-IPN, México City).

APPENDIX: STATIC PROPERTIES

For immediate reference, in this appendix we quote the expressions for the static properties $\chi(k)$, $L^0(k)$, $\chi^S(k)$, and $L_S^0(k)$ associated with $F(k,z)$ and $F_S(k,z)$ [see Eqs. (1)–(4)] in terms of the two- and three-particle correlation functions, $g(r)$ and $g^{(3)}(\mathbf{r},\mathbf{r}')$. For the details of their derivation, we refer the reader to the original source, namely, Ref. [5]. These expressions are

$$\chi(k)=\left(\frac{k_BT}{m}\right)^2\left[1+n\int d\mathbf{r}g(r)\frac{\partial^2\beta u(r)}{\partial z^2}\left(\frac{1-\cos(kz)}{k^2}\right)-\frac{1}{S(k)}\right], \tag{A1}$$

$$\begin{aligned}M^2\beta^2L^0(k)=nD_0\int d^3rg(r)\frac{\partial^2\beta u(r)}{\partial z^2}[1+2\cos kz]-\frac{D_0n^2}{k^2}\left[\int d^3rg(r)\frac{\partial^2\beta u(r)}{\partial z^2}(1-\cos kz)\right]^2\\ +\frac{2D_0n}{k}\int d^3rg(r)\frac{\partial^3\beta u(r)}{\partial z^3}\sin kz+\frac{2D_0n}{k^2}\int d^3rg(r)(1-\cos kz)\left[\frac{\partial\nabla\beta u(r)}{\partial z}\right]^2\\ +\frac{D_0n^2}{k^2}\int d^3rd^3r'g(\mathbf{r},\mathbf{r}')\{1-2\cos kz+\cos[k(z-z')]\}\left[\frac{\partial\nabla\beta u(r)}{\partial z}\right]\left[\frac{\partial\nabla'\beta u(r')}{\partial z'}\right],\end{aligned} \tag{A2}$$

$$\chi^{(S)}(k)=\frac{(k_BT/M)^2}{k^2}\left[n\int d\mathbf{r}g(r)\frac{\partial^2\beta u(r)}{\partial z^2}\right], \tag{A3}$$

and

$$\begin{aligned}k^2M^2\beta^2L_S^0(k)=k^2D_0\left[n\int d\mathbf{r}g(r)\frac{\partial^2\beta u(r)}{\partial z^2}\right]\\ -D_0n^2\left[\int d^3rg(r)\frac{\partial^2\beta u(r)}{\partial z^2}\right]^2\\ +2D_0n\int d^3rg(r)\left[\frac{\partial\nabla\beta u(r)}{\partial z}\right]^2\\ +D_0n^2\int d^3rd^3r'g(\mathbf{r},\mathbf{r}')\left[\frac{\partial\nabla\beta u(r)}{\partial z}\right]\\ \times\left[\frac{\partial\nabla'\beta u(r')}{\partial z'}\right].\end{aligned} \tag{A4}$$

In the equations above, $u(r)$ is the effective interaction pair potential between colloidal particles. Finally, we should repeat that in this paper we have systematically dropped the subindex "UU" employed in Ref. [5], where $\chi(k)$, $\chi^{(S)}(k)$,

$L^0(k)$, and $L_S^0(k)$ are denoted, respectively, by $\chi_{UU}(k)$, $\chi_{UU}^{(S)}(k)$, $L_{UU}(k)$, and $L_{UU}^{(S)}(k)$.

The integral involving $g^{(3)}(\mathbf{r},\mathbf{r}')$ in the last term of Eq. (A2) was evaluated, in practice, introducing the use of Kirkwood's superposition approximation, $g^{(3)}(\mathbf{r},\mathbf{r}') \approx g(r)g(r')g(|\mathbf{r}-\mathbf{r}'|)$, plus the additional simplification of approximating $g(|\mathbf{r}-\mathbf{r}'|)$ by its asymptotic value of 1. This leads to replacing the integral

$$\Delta m^{(3)}(k) \equiv \int d\mathbf{r}' d\mathbf{r} g(\mathbf{r},\mathbf{r}')(1-2\cos(\mathbf{k}\cdot\mathbf{r}) + \cos\{[\mathbf{k}\cdot(\mathbf{r}-\mathbf{r}']\})(\mathbf{k}\cdot\nabla)(\mathbf{k}\cdot\nabla') \times(\nabla\cdot\nabla')\beta u(r)\beta u(r') \quad \text{(A5)}$$

by

$$\Delta m^{(3)}(k) = \left[\int d\mathbf{r} g(r)[1-\cos(\mathbf{k}\cdot\mathbf{r})](\mathbf{k}\cdot\nabla)\nabla\beta u(\mathbf{r})\right]^2. \quad \text{(A6)}$$

The corresponding approximate expressions for the case of self-diffusion are identical, ignoring the term involving $\cos(\mathbf{k}\cdot\mathbf{r})$ in these two equations. Thus, within these approximations, the only static input needed by the SCGLE theory is $g(r)$.

[1] P. N. Pusey, in *Liquids, Freezing and the Glass Transition*, edited by J. P. Hansen, D. Levesque, and J. Zinn-Justin (Elsevier, Amsterdam, 1991).
[2] G. Nägele, Phys. Rep. **272**, 215 (1996).
[3] L. Yeomans-Reyna and M. Medina-Noyola, Phys. Rev. E **64**, 066114 (2001).
[4] L. Yeomans-Reyna, H. Acuña-Campa, and M. Medina-Noyola, Phys. Rev. E **62**, 3395 (2000).
[5] L. Yeomans-Reyna and M. Medina-Noyola, Phys. Rev. E **62**, 3382 (2000).
[6] W. Hess and R. Klein, Adv. Phys. **32**, 173 (1983).
[7] (a) W. Götze and E. Leutheusser, Phys. Rev. A **11**, 2173 (1975); (b) W. Götze, E. Leutheusser, and S. Yip, *ibid.* **23**, 2634 (1981).
[8] W. Götze, in *Liquids, Freezing and Glass Transition*, edited by J. P. Hansen, D. Levesque, and J. Zinn-Justin (North-Holland, Amsterdam, 1991).
[9] N.J. Wagner, Phys. Rev. E **49**, 376 (1994).
[10] (a) G. Nägele, J. Bergenholtz, and J.K.G. Dhont, J. Chem. Phys. **110**, 7037 (1999); (b) G. Nägele and J. Bergenholtz, *ibid.* **108**, 9893 (1998).
[11] (a) G. Nägele and J.K.G. Dhont, J. Chem. Phys. **108**, 9566 (1998); (b) G. Nägele and P. Baur, Physica A **245**, 297 (1997).
[12] A.J. Banchio, J. Bergenholtz, and G. Nägele, J. Chem. Phys. **113**, 3381 (2000).
[13] A.J. Banchio, J. Bergenholtz, and G. Nägele, Phys. Rev. Lett. **82**, 1792 (1999).
[14] (a) R. Verberg, I.M. de Schepper, and E.G.D. Cohen, Phys. Rev. E **61**, 2967 (2000); (b) E.G.D. Cohen and I.M. de Schepper, J. Stat. Phys. **63**, 242 (1991); (c) I.M. de Schepper, E.G.D. Cohen, P.N. Pusey, and H.N.W. Lekkerkerker, J. Phys.: Condens. Matter **1**, 6503 (1989).
[15] B. Cichocki and B.U. Felderhof, Physica A **204**, 152 (1994).
[16] M. Medina-Noyola, Faraday Discuss. Chem. Soc. **83**, 21 (1987).
[17] M. Medina-Noyola and J.L. del Rio-Correa, Physica A **146**, 483 (1987).
[18] G.H. Vineyard, Phys. Rev. **110**, 999 (1958).
[19] J. P. Hansen and I. R. McDonald, *Theory of Simple Liquid* (Academic, New York, 1976).
[20] J. L. Boon and S. Yip, *Molecular Hydrodynamics* (Dover, New York, 1980).
[21] (a) J.L. Arauz-Lara and M. Medina-Noyola, Physica A **122**, 547 (983); (b) G. Nägele, M. Medina-Noyola, R. Klein, and J.L. Arauz-Lara, *ibid.* **149**, 123 (1988).
[22] H. Acuña-Campa and M. Medina-Noyola, J. Chem. Phys. **113**, 869 (2000).
[23] P.N. Pusey and R.J.A. Tough, J. Phys. A **15**, 1291 (1982).
[24] J.L. Arauz-Lara and M. Medina-Noyola, Physica A **122**, 547 (1983).
[25] J. Santana-Solano and J.L. Arauz-Lara, Phys. Rev. Lett. **87**, 038302 (2001).
[26] M. P. Allen and D. J. Tildesley, *Computer Simulation of Liquids* (Oxford University Press, New York, 1987).
[27] D.L. Ermak and J.A. McCammon, J. Chem. Phys. **69**, 1352 (1978).
[28] K.J. Gaylor, I.K. Snook, W. van Megen, and R.O. Watts, J. Phys. A **13**, 2513 (1980).
[29] K. Zahn, J.M. Méndez-Alcaraz, and G. Maret, Phys. Rev. Lett. **79**, 175 (1997).
[30] E. J. W. Verwey and J. T. G. Overbeck, *Theory of the Stability of Lyophobic Colloids* (Elsevier, Amsterdam, 1948).
[31] M. Medina-Noyola and D.A. McQuarrie, J. Chem. Phys. **73**, 6229 (1980).
[32] W. Härtl, H. Versmold, U. Witting, and P. Linse, J. Chem. Phys. **97**, 7797 (1992).
[33] F. de J. Guevara-Rodríguez and M. Medina-Noyola (unpublished).
[34] L. Yeomans-Reyna, F. de J. Guevara-Rodríguez, H. Acuña-Campa, and M. Medina-Noyola (unpublished).